p53 Transgenic Mice Are Highly Susceptible to 4-Nitroquinoline-1-Oxide-Induced Oral Cancer

Zhongqiu Zhang,[1] Yian Wang,[1] Ruisheng Yao,[1] Ronald A. Lubet,[2] and Ming You[1]

[1]Department of Surgery, Washington University School of Medicine, St. Louis, Missouri and [2]Chemoprevention Agent Development Research Group, National Cancer Institute, Bethesda, Maryland

Abstract

In this study, we did a bioassay employing mice with a dominant-negative p53 mutation ($p53^{Val135/WT}$) to assess whether a germ-line p53 mutation predisposed mice toward the development of squamous cell carcinomas (SCC) in the oral cavity. Treatment of the mouse oral cavity with 4-nitroquinoline-1-oxide produced a 66%, 91%, and 20% tumor incidence in the oral cavity, esophagus, and forestomach/stomach, respectively, in $p53^{Val135/WT}$ mice. In contrast, only a 25%, 58%, and 4% tumor incidence was observed in oral cavity, esophagus, and forestomach/stomach, respectively, in wild-type littermates ($p53^{WT/WT}$). The most striking difference between $p53^{Val135/WT}$ and $p53^{WT/WT}$ mice following the carcinogen treatment was the higher prevalence and more rapid development of SSC in $p53^{Val135/WT}$ mice than in wild-type mice. To identify the precise genes or pathways involved in these differences during tumor development, we examined gene expression profiles of 4-nitroquinoline-1-oxide-treated normal tongues as well as tongue SCC in $p53^{Val135/WT}$ and $p53^{WT/WT}$ mice. Microarray and GenMAPP analysis revealed that dominant-negative p53 (^{135}Valp53) affects several cellular processes involved in SCC development. Affected processes included apoptosis and cell cycle arrest pathways, which were modulated in both tumor and normal epithelium. These results showed that reduction of p53-dependent apoptosis and increases in cell proliferation might contribute to the observed increase in oral cavity and gastroesophageal malignancies in $p53^{Val135/WT}$ mice as well as to the more rapid growth and progression of tumors.
(Mol Cancer Res 2006;4(6):401–10)

Introduction

Head and neck cancer accounts for 3% to 5% of all malignancies in Western countries, with cancer of the oral cavity accounting for 30% of all head and neck cancers. Squamous cell carcinoma (SCC) of the oral cavity is the sixth most frequent cancer in the world and ~30,000 new cases are diagnosed annually in the United States (1). The development of oral SCC shows a positive correlation with exposure to tobacco and alcohol. Multiple genetic changes are thought to contribute to the development of SCCs of oral cavity (2-5).

The molecular pathways involved in the development of oral SCC are poorly understood. Mutations in the *p53* gene are the most prevalent mutations in human cancer and can be sporadic or germ-line in nature (6, 7). The p53 protein is present in normal cells and induces cell cycle arrest or apoptosis in the presence of DNA damage. Mutant p53 protein lacks this property. Germ-line mutations in p53 are associated with the Li-Fraumeni family cancer syndrome, which predisposes individuals to multiple, unpredictable, aggressive, and often lethal tumors (8). We have shown previously that p53 transgenic mice with a dominant-negative p53 mutation are highly susceptible to carcinogen-induced lung adenoma/adenocarcinoma, uterine sarcoma, and colon adenocarcinoma (9-12). Mutation in the *p53* gene is also commonly seen in SCCs of oral mucosa (13-16). Abnormal staining of p53 protein is a frequent finding (17-19).

The objective of this study was to determine the role of *p53* tumor suppressor in mouse oral SCC development. A bioassay using dominant-negative p53 transgenic ($p53^{Val135/WT}$) mice was done to assess if there is a correlation between germ-line *p53* mutation and susceptibility toward SCC in the oral cavity. Treatment of mouse oral epithelia with 4-nitroquinoline-1-oxide (4NQO) is a well-established model for human head and neck SCCs (20, 21). The developing tumors are moderate to well-differentiated SCCs that morphologically resemble human tumors (19). We found that p53 transgenic mice are highly susceptible to 4NQO-induced oral cancer and that the resulting tumors are more likely to progress. In addition, we examined that the molecular pathways involved in the tumor development include apoptosis and cell cycle arrest.

Received 2/1/06; revised 3/28/06; accepted 4/13/06.
Grant support: NIH grants R01CA58554 and N01CN25104.
The costs of publication of this article were defrayed in part by the payment of page charges. This article must therefore be hereby marked advertisement in accordance with 18 U.S.C. Section 1734 solely to indicate this fact.
Note: Z. Zhang and Y. Wang contributed equally to this work.
Requests for reprints: Ming You, Department of Surgery, Washington University School of Medicine, 660 South Euclid Avenue, St. Louis, MO 63110. Phone: 314-462-9294; Fax: 314-362-9366. E-mail: youm@wustl.edu

doi:10.1158/1541-7786.MCR-06-0028

Results

Effect of p53 Germ-line Mutation (Ala^{135}Val) on 4NQO-Induced Tumorigenesis

To determine whether the $p53^{Val135/WT}$ mice would be more susceptible to chemical induction of upper gastrointestinal tumors than wild-type littermates, a 4NQO-induced tumor bioassay was conducted. Six-week-old $p53^{Val135/WT}$ and $p53^{WT/WT}$ mice were treated with 4NQO. After 16 weeks of

treatment and 32 weeks postinitiation, $p53^{Val135/WT}$ mice had developed significantly more and larger upper gastrointestinal tumors, including oral cavity, esophagus, and forestomach/stomach tumors, than their $p53^{WT/WT}$ counterparts.

As shown in Table 1 and Fig. 1A, in 4NQO-treated groups, the survival rate of wild-type mice was significantly higher than the p53 transgenic mice. Most $p53^{Val135/WT}$ mice were either dead or moribund before the end of the experiment due to advanced oral/upper gastrointestinal tumors. All tumor phenotypes, including those from the mice either dead or moribund, were included in Table 1. As shown in Table 1, treatment of $p53^{Val135/WT}$ mice with 4NQO produced more than 66%, 91%, and 20% incidences of oral mucosa, esophagus, and forestomach/stomach tumors, respectively, whereas only 25%, 58%, and 4% tumor incidences were observed in the oral mucosa, esophagus, and forestomach/stomach, respectively, in wild-type mice treated with the same carcinogen (Table 1). 4NQO produced an average of ~0.3 tongue SCC and ~1.0 esophageal SCC in $p53^{WT/WT}$ mice, whereas treatment of $p53^{Val135/WT}$ mice produced an average of ~1.0 tongue SCC and ~3.2 esophageal SCC (Table 1).

Morphologically, oral cavity lesions included lip, tongue, palate, and larynx tumors. Some tumors were grossly enlarged with invasion to surrounding tissues. In some advanced cases in the $p53^{Val135/WT}$ group, the entire oral cavity was diffusely swollen and the bottom of the oral cavity was grossly enlarged, with head and neck lymph node involvement. Sometimes, enlarged oral SCC could be easily palpated through the neck or protruded through the mouth. Histopathologically, these tumors were oral cavity, esophageal, and forestomach SCCs (Fig. 1B). Most SCCs showed proliferation into the submucosa and exhibited features of squamous cell differentiation, such as keratin pearls. The majority of $p53^{Val135/WT}$ mice developed tumors more rapidly than the wild-type mice and the tumors displayed more obvious features of malignancy, including large size, lymph node involvement, more nuclear atypia, and invasiveness. Furthermore, histopathology data showed that SCCs had relatively poorly differentiated cells in $p53^{Val135/WT}$ tumors when compared with $p53^{WT/WT}$ tumors. Some poorly differentiated SCCs are composed of spindle-shaped cells and show no keratinization. No tumors were found in either $p53^{WT/WT}$ or $p53^{Val135/WT}$ vehicle control mice. Because spontaneous upper gastrointestinal tumors are rare in mice, $p53^{Val135/WT}$ mice have an increased susceptibility to 4NQO-induced oral and upper gastrointestinal SCCs. No significant differences between the body weights of any of the groups treated with 4NQO compared with controls occurred in either experiment. However, the majority of $p53^{Val135/WT}$ mice were terminated before the end of the experiment due to overt SCCs. The survivorship data are shown in Fig. 1A.

Microarray Analysis of Normal and Tumor Tissues from Tongues Treated with 4NQO

To identify the precise genes or pathways responsible for these differences in tumor susceptibility and growth, four to five normal and tumor samples from both $p53^{WT/WT}$ and $p53^{Val135/WT}$ groups were examined. In normal tongue tissues, microarray analysis revealed 271 genes differentially expressed between $p53^{WT/WT}$ and $p53^{Val135/WT}$ mice treated with 4NQO. Among them, 67 genes were underexpressed, whereas 204 genes were overexpressed in $p53^{Val135/WT}$ normal tissues when using 2-fold change and $P < 0.05$ (t test) as cutoff (Fig. 2A). Moreover, when we compared the expression of tongue SCCs, 913 genes were found, which showed differential expression between $p53^{WT/WT}$ and $p53^{Val135/WT}$ tumors. Among them, 377 genes were underexpressed, whereas 536 genes were overexpressed in $p53^{Val135/WT}$ tumors (Table 2; Fig. 2B). We also ranked the genes in the normal-to-normal and tumor-to-tumor comparisons based on fold expression difference in Tables 3 and 4. We then verified the finding from microarray analysis that the expression of *Rassf1A* was decreased in tumors from $p53^{Val135/WT}$ mice when compared with those from $p53^{WT/WT}$ mice. We conducted methylation-specific PCR (MSP) analysis to obtain a methylation profile of *Rassf1A* in SCC. As shown in Fig. 3, 25% of tumors from $p53^{WT/WT}$ mice and 75% of the tumors from $p53^{Val135/WT}$ mice showed *Rassf1A* promoter methylation. No *Rassf1A* methylation was detected in paired normal tissues. These results indicate a correlation between array data and hypermethylation status of the *Rassf1A* gene in SCC (Table 2).

Finally, we used GenMAPP to illustrate all the available pathways containing differentially expressed genes associated with p53 status in tongue tumorigenesis. Several cellular pathways, such as apoptosis, cell cycle, transforming growth factor-β, and Ras-mitogen-activated protein kinase pathways, showed alterations in both 4NQO-treated normal tissue and

Table 1. 4NQO-Induced Tumorigenesis in p53 Transgenic ($p53^{Val135/WT}$) Mice

Group	Genotype	*n*	Treatment*	Tumor incidence (%)			Tumor multiplicity	
				Oral cavity	Esophagus	Forestomach/stomach	Oral cavity	Esophagus
1	$p53^{WT/WT}$	12	Vehicle	0	0/12 (0)	0/12 (0)	0	0
2	$p53^{Val135/WT}$	12	Vehicle	0	0/12 (0)	0/12 (0)	0	0
3	$p53^{WT/WT}$	24	4NQO	6/24 (25.0)	14/24 (58.3)	1/24 (4.2)	0.3 ± 0.5	1.0 ± 1.0
4	$p53^{Val135/WT}$	24	4NQO	16/24 (66.7)†	22/24 (91.7)†	5/24 (20.8)	1.0 ± 0.9‡	3.2 ± 2.0‡

*Approximately equal numbers of males and females were used, with no significant difference in tumor multiplicity between the sexes. At age 6 weeks, mice in groups 1 and 2 were given vehicle. Mice in groups 3 and 4 were given 4NQO (5 mg/mL in propylene glycol) thrice weekly for 16 weeks. All animals were terminated 32 weeks after last dose 4NQO treatment.

†$P < 0.05$, tumor incidence in $p53^{Val135/WT}$ mice (group 4) was significantly different from that of $p53^{WT/WT}$ mice (group 3; Fisher's exact test).

‡$P < 0.001$, tumor multiplicity in $p53^{Val135/WT}$ mice (group 4) was significantly different from that of $p53^{WT/WT}$ mice (group 3; Wilcoxon's rank-sum test).

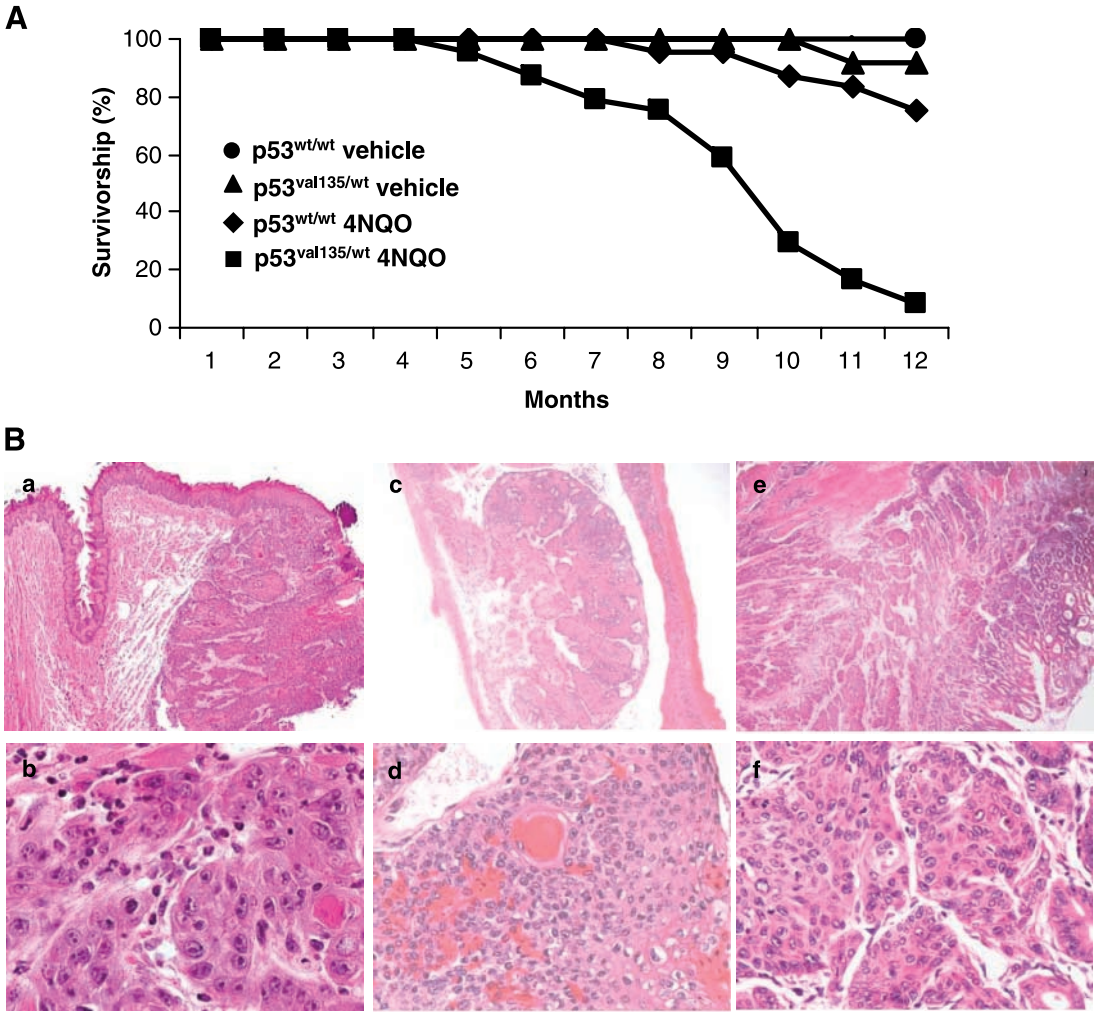

FIGURE 1. 4NQO-induced mouse tongue tumorigenesis in $p53^{Val135/WT}$ and $p53^{WT/WT}$ mice. **A.** Survivorship of $p53^{Val135/WT}$ and $p53^{WT/WT}$ mice treated with 4NQO. Six-week-old UL53-3 mice were randomized into four groups according to the p53 genotypes ($p53^{WT/WT}$ or $p53^{Val135/WT}$). All mice were treated with 4NQO or vehicle control thrice weekly for 16 weeks. The experiment was terminated 32 weeks after the last treatment with 4NQO. **B.** Histopathology of 4NQO-induced tumors in $p53^{Val135/WT}$ mice. **a** and **b,** light photomicrographs of tongue SCC at ×40 and ×400 magnification from $p53^{Val135/WT}$ mice, respectively; **c** and **d,** light photomicrographs of esophageal SCC at ×40 and ×400 magnification from $p53^{Val135/WT}$ mice, respectively; **e** and **f,** light photomicrographs of forestomach SCC at ×40 and ×400 magnification from $p53^{Val135/WT}$ mice, respectively.

tumors from $p53^{WT/WT}$ versus $p53^{Val135/WT}$ mice. Among them, the cell cycle and apoptotic signaling pathways played an important role in 4NQO-induced tongue tumorigenesis. As shown in the cell cycle regulation pathway (Fig. 4A), the expression of p53, Atm, Bub1, Tgfb1, Cdc25b, Orc21, and Cdc7 was differentially expressed in normal tissues of $p53^{WT/WT}$ versus $p53^{Val135/WT}$ mice. In addition, the expression Mdm2, Ccna1, Abl1, and Tfdp1 was differentially expressed in tumors of $p53^{WT/WT}$ versus $p53^{Val135/WT}$ mice. In the apoptotic pathways, expression of Bid and p53 was altered in normal tissues of the $p53^{Val135/WT}$ mice, whereas several death receptors or activators of cell death, such as Tnf, Tnfsf10, Prf1, Tradd, Ripk1, Apaf1, Mdm2, Bcl2, and Casp7, were found altered in $p53^{Val135/WT}$ tumors (Fig. 4B). These results indicate that deregulation of cell cycle and reduction of apoptosis activity may, in part, contribute to the increased oral malignancy in $p53^{Val135/WT}$ mice on carcinogen exposure.

Discussion

In the present study, we induced upper gastrointestinal malignancy with the carcinogen 4NQO, which was documented to induce oral cavity tumors in various species and multiple strains of mice (20-22). Using p53 transgenic mice, we found that introduction of a dominant-negative p53 mutant ($Ala^{135}Val$) into the germ-line significantly enhanced tumorigenesis in the oral mucosa and upper gastrointestinal system on 4NQO treatment. The most striking distinction between $p53^{Val135/WT}$ and $p53^{WT/WT}$ mice on carcinogen treatment was that the majority of $p53^{Val135/WT}$ mice developed tumors more rapidly than the wild-type mice and the tumors displayed more obvious histologic features of malignancy. Thus, at 9 months following the initial 4NQO treatment, ~60% of the $p53^{Val135/WT}$ mice had died, whereas <15% of the $p53^{WT/WT}$ mice had died. In contrast, survival was >95% for control mice of either genotype. This implies that the mutant p53 allele

greatly increased SCC susceptibility possibly through a promotion function of the missense protein. The wild-type p53 protein facilitates the regulation of genomic stability by preventing cell cycle entry and initiates apoptotic cell death in response to DNA damage (23, 24). Thus, loss of normal function of p53 leads to deregulation of the cell cycle and continued cell cycle progression after DNA damage resulting in accumulation of genetic damage. Our results strongly suggest that p53 plays a role in proliferation and apoptosis of squamous cells exposed to chemical carcinogens. Altered p53 protein expression has been associated with increased proliferative rates in other tumors, such as human breast cancer (25). The observation in this study is the profound effect of the mutant p53 transgene on development of upper gastrointestinal SCC in $p53^{Val135/WT}$ mice, strongly indicating that upper gastrointestinal SCC formation is highly p53 dependent.

Our findings are consistent with the results from Gallo et al. (26) in which they detected a germ-line p53 mutation in head and neck cancer patients with multiple malignancies and in their first-degree relatives. In addition, Rowley et al. (27) and Qin et al. (28) reported that the *p53* gene is an early target for mutation in oral tumor development, with mutations being detected in 40% to 50% of premalignant lesions and SCCs. More recently, Ide et al. (29) found that p53 haploinsufficiency profoundly accelerates the onset of tongue tumors in mice lacking the xeroderma pigmentosum group A gene. All together, these results suggest that p53 plays a major and early role in head and neck tumor development. Our finding would seem to make this *in situ* mouse model particularly relevant for studying the role of p53 in head and neck tumorigenesis as well as for screening potential preventive or therapeutic agents for head and neck cancer.

To profile genes or pathways responsible for enhanced susceptibility to SCC in the oral cavity on 4NQO induction as well as the more rapid tumor growth and progression, altered gene expression in tongue tumors and normal tissues was investigated. Microarray studies with the GenMAPP analysis revealed that germ-line p53 mutation affects several cellular processes involved in the tumorigenesis possibly through the interplay among apoptosis, cell cycle arrest, transforming growth factor-β signaling pathway, and Ras-mitogen-activated protein kinase pathway. For example, our data showed that wild-type p53 expression levels in both normal and tumor tissues were significantly decreased in $p53^{Val135/WT}$ mice, which regulate multiple cell type–dependent intracellular and cellular events. Thus, cross-talk of these cellular processes may be involved in the tumorigenic process itself. Furthermore, microarray results showed that cell proliferation significantly increased, whereas apoptosis activity decreased in $p53^{Val135/WT}$ samples compared with that from $p53^{WT/WT}$ mice. On exposure $p53^{Val135/WT}$ mice to 4NQO, the wild-type p53 could not function properly because of the dominant-negative effect of the mutant transgene, resulting in higher cell proliferation and decreased apoptosis relative to $p53^{WT/WT}$ mice. In $p53^{WT/WT}$ mice, high

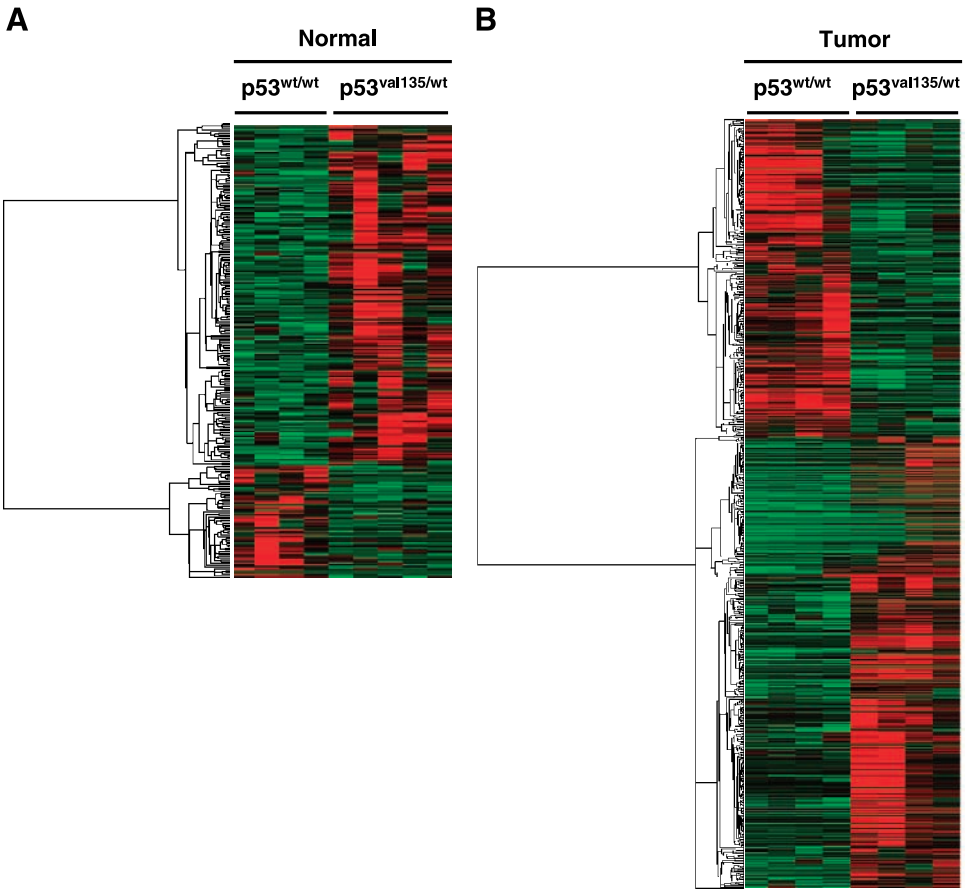

FIGURE 2. Microarray analysis 4NQO-induced mouse tongue tumors. **A.** Differentially expressed genes found in normal tissues of $p53^{Val135/WT}$ mice. More than 271 differentially expressed genes were detected in normal tongue tissues induced by 4NQO; 67 genes were underexpressed and 204 genes were overexpressed in $p53^{Val135/WT}$ mice. Green, expression below the mean for the gene; black, near the mean; red, above the mean. **B.** Differentially expressed genes found in tumors of $p53^{Val135/WT}$ mice. Over 913 differentially expressed genes were detected in tongue SCCs induced by 4NQO; 377 genes were underexpressed and 536 genes were overexpressed in $p53^{Val135/WT}$ mice.

Table 2. Microarray Analysis for Differentially Expressed Genes between $p53^{WT/WT}$ and $p53^{Val135/WT}$ in Early and Later Stages from Mouse Oral Tumorigenesis

Genbank	Gene name	Symbol	Fold change ($P < 0.05$) $p53^{WT/WT}/p53^{Val135/WT}$	
			Normal	Tumor
Apoptosis-related genes				
AB021961	*Transformation-related protein 53*	Trp53	−9.6	−14.6
U75506	*BH3-interacting domain death agonist*	Bid	3.5	−2.5
L31532	*Bcl-2α gene, exon 2*	Bcl2		−2.1
D86353	*Caspase-7*	Casp7		−2.0
AJ224738	*CASP2 and RIPK1 domain containing adaptor with death domain*	Cradd		−2.4
D84196	*TNFA gene for tumor necrosis factor-α*	TNFA		−4.4
U37522	*Tumor necrosis factor (ligand) superfamily, member 10*	Tnfsf10		−2.8
M21065	*IFN-regulatory factor 1*	Irf1		−4.2
AI853773	*F-box only protein 21*	Fbxo21		−2.0
U73037	*IFN-regulatory factor 7*	Irf7		−11.5
AV292430	*IFN-regulatory factor 3*	Irf3		−2.9
L26479	*Eukaryotic translation elongation factor 1 α2*	Eef1a2		−2.3
AF047699	*Fragile histidine triad gene*	Fhit		1.9
Cell cycle and growth-related genes				
X57800	*PCNA gene for proliferating cell nuclear antigen*	Pcna	−1.4	−1.9
U59758	*p53-variant (p53) mRNA*		−4.2	−4.1
U36760	*Forkhead box G1*	Foxg1	5.1	−7.0
AW048394	*Transformation-related protein 53-binding protein 1*	Trp53bp1	−2.1	
AA940503	*Cell division cycle 23*	Cdc23	−2.4	
AV094683	*Origin recognition complex, subunit 2-like (Saccharomyces cerevisiae)*	Orc21	−3.5	
D87326	*Germ cell–specific gene 2*	Gsg2	−2.8	
D87271	*ERK2 gene for extracellular signal-regulated kinase 2*	ERK2	2.9	
X90648	*v-crk sarcoma virus CT10 oncogene homologue (avian) like*	Crkl	−2.6	
AA089181	*Papillary renal cell carcinoma (translocation associated)*	Prcc	−2.0	
U33629	*Myeloid ecotropic viral integration site 1*	Meis1	2.1	
X84311	*Cyclin A1*	Ccna1		4.6
AI849928	*Cyclin D1*	Ccnd1		−2.2
U95826	*Cyclin G2*	Ccng2		2.4
X61940	*Dual-specificity phosphatase 1*	Dusp1		2.6
AV086728	*NIMA (never in mitosis gene a)–related expressed kinase 1*	Nek1		−2.4
AV138783	*Growth arrest and DNA damage-inducible 45β*	Gadd45b		2.7
U60884	*Bridging integrator 1*	Bin1		−2.4
X95503	*Pleiomorphic adenoma gene-like 1*	Plagl1		−2.2
AF076845	*Hus1 homologue (Schizosaccharomyces pombe)*	Hus1		2.0
AI842328	*Calmodulin 2*	Calm2		−2.0
M21828	*Growth arrest specific 2*	Gas2		−2.0
AJ010108	*Adenylate kinase 1*	Ak1		−2.4
AF043939	*Cell cycle regulatory transcription factor DP1 gene*	DP1		−2.1
U67187	*Regulator of G-protein signaling 2*	Rgs2		2.5
D30782	*Epiregulin*	Ereg		6.0
AI835443	*Brain-expressed myelocytomatosis oncogene*	Bmyc		−2.1
AF019249	*N-myc (and STAT) interactor*	Nmi		−2.2
AB033921	*N-myc downstream regulated 2*	Ndr2		−3.4
AA833077	*Myc-induced nuclear antigen*	Mina		2.4
X13945	*L-myc gene*	Lmyc		−2.2
U32394	*Max dimerization protein 3*	Mad3		2.6
U32395	*Max dimerization protein 4*	Mad4		−2.1
D14849	*Meiosis-specific nuclear structural protein 1*	Mns1		−3.6
AV317327	*Mitogen-activated protein kinase 1*	Mapk1		3.2
D11374	*Signal-induced proliferation associated gene 1*	Sipa1		−3.3
U02487	*Sarcospan*	Sspn		−2.2
M95200	*Vascular endothelial growth factor A*	Vegfa		−3.8
AV240218	*Avian reticuloendotheliosis viral (v-rel) oncogene related B*	Relb		−2.0
D13759	*Mitogen-activated protein kinase kinase kinase 8*	Map3k8		2.5
X07750	*Thyroid hormone receptor α*	Thra		−2.4
X55957	*Inhibin α*	Inha		−2.3
X96639	*Exostoses (multiple) 1*	Ext1		−2.6
AI838195	*Opioid growth factor receptor*	Ogfr		−3.5
X69620	*Inhibin β-B*	Inhbb		−5.6
X99572	*c-fos-induced growth factor*	Figf		−2.6
M29464	*Platelet-derived growth factor, α*	Pdgfa		−2.0
M37823	*Fibroblast growth factor-5 DNA, exon 3*	Fgf5		2.1
U22445	*Thymoma viral proto-oncogene 2*	Akt2		−2.6
U19860	*Growth arrest specific 7*	Gas7		2.3
U08337	*Growth differentiation factor 5*	Gdf5		2.0
M70642	*Connective tissue growth factor*	Ctgf		−2.3
Small GTPase-related genes				
AI788669	*ADP-ribosylation factor 6*	Arf6	2.1	

(*Continued on the following page*)

Table 2. Microarray Analysis for Differentially Expressed Genes between $p53^{WT/WT}$ and $p53^{Val135/WT}$ in Early and Later Stages from Mouse Oral Tumorigenesis (Cont'd)

Genbank	Gene name	Symbol	Fold change ($P < 0.05$) $p53^{WT/WT}/p53^{Val135/WT}$	
			Normal	Tumor
AA178600	*Ras association (RalGDS/AF-6) domain family 2*	Rassf2	−2.3	
AF053959	*Ras association (RalGDS/AF-6) domain family 5*	Rassf5	1.7	
AV345884	*Ral guanine nucleotide dissociation stimulator*	Ralgds	−2.3	
X70804	*RAB17, member RAS oncogene family*	Rab17	−2.6	
AW122347	*Rac GTPase-activating protein 1*	Racgap1	2.0	
C76597	*Rho GTPase-activating protein 29*		−4.4	
AI850288	*Rhophilin, Rho GTPase-binding protein 2*	Rhpn2		2.2
U73941	*Rap2-interacting protein*	Rap2ip		2.1
AF016482	*Ras homologue N (RhoN)*	Arhn		−2.1
AV043011	*RAS-like, family 2, locus 9*	Rasl2-9		−2.1
AI838152	*Nischarin*	Nisch		−2.0
U53219	*IFN-γ-induced GTPase*	Igtp		−13.4
AJ007971	*IFN-inducible GTPase 1*	Iigp1		−28.8
AJ007972	*IFN-inducible GTPase 2*	Igtp		−4.5
D50500	*RAB11a, member RAS oncogene family*	Rab11a		2.3
AW049415	*Ras association (RalGDS/AF-6) domain family 1*	Rassf1	1.6	−1.4

levels of wild-type p53 protein were induced, resulting in cell cycle arrest that should subsequently allow cells to recover from damage or undergo apoptosis. These results suggested that reduction of p53-dependent cell cycle inhibition and apoptosis might contribute to the observed increase in upper gastrointestinal tumor incidence in $p53^{Val135/WT}$ mice.

In summary, the present study and our previous *in vivo* studies have shown that *in situ* tumors with a germ-line p53 mutation can be induced in a variety of organ sites, including lung, uterus, colon, and upper gastrointestinal system (9-12). Microarray analyses began to offer clues for the mechanisms of tumor development associated with inactivation of p53. Our findings show that the combined use of mice with a dominant-negative p53 mutation combined with the carcinogen 4NQO yields a model of SCC of the upper gastrointestinal tract system that seems relevant to human oral SCC.

Materials and Methods

Agent

The chemical carcinogen 4NQO (Sigma Chemical Co., St. Louis, MO) was dissolved in propylene glycol to a final concentration of 5 mg/mL. The solution was stored at 4°C and a fresh aliquot was used each application session.

Animals

$p53^{Val135/WT}$ mice carrying a ^{135}Valp53 mutation in exon 5 were obtained from the National Institute of Environmental Health Sciences (Research Triangle Park, NC). Mice were housed four per cage in plastic cages with hardwood bedding and dust covers in a HEPA-filtered, environmentally controlled room (24 ± 1°C with a 12-hour light/12-hour dark cycle).

p53 Genotype

$p53^{Val135/WT}$ mice were developed by microinjection of FVB/J mouse oocytes with a BALB/c mouse genomic clone of the *p53* gene containing a point mutation in codon 135 (Ala-to-Val) at exon 5. The mutation, a C-to-T transition, created a RFLP with a new *Hph*I restriction enzyme cleavage site (recognition site: GGTGA). This mutation was used to genotype $p53^{Val135/WT}$ mice using PCR-RFLP method as described previously (9).

Tumor Development

Six-week-old $p53^{Val135/WT}$ mice were randomized into four groups according to the p53 genotypes (Table 1). Mice in groups 3 and 4 were lightly anesthetized by inhalation of methoxyflurane vapor. The palate was stroked once from the soft palate to the incisive papilla with a no. 3 camel hairbrush, which had been dipped once in 4NQO solution. Mice in groups 1 and 2 were given vehicle control (propylene glycol). All mice were treated by direct application thrice weekly for 16 weeks. Thirty-two weeks after the last treatment with 4NQO, animals from all four groups were euthanized by CO_2 asphyxiation. A portion of the upper gastrointestinal tumors and normal tissues were isolated, placed in individual tubes, and immediately frozen in liquid nitrogen. The remaining tumors and normal tissues were fixed in 10% neutral-buffered formalin overnight followed by 70% ethanol and paraffin embedding. Tissue sections (5 μm) were stained with H&E for histopathologic evaluation. A gross necropsy was done.

RNA Isolation and Amplification

Total RNA from each sample was isolated by Trizol (Invitrogen, Carlsbad, CA) and purified using the RNeasy Mini kit and RNase-free DNase Set (Qiagen, Valencia, CA) according to the manufacturer's protocols. *In vitro* transcription-based RNA amplification was then done on each sample. cDNA for each sample was synthesized using a SuperScript cDNA Synthesis kit (Invitrogen, Carlsbad, CA) and a T7-$(dT)_{24}$ primer: 5′-GGCCAGTGAATTGTAATACGACTCACTA-TAGGGAGGCGG-$(dT)_{24}$-3′. The cDNA was cleaned using phase-lock gel (Fisher, Hampton, NH) phenol/chloroform extraction. Then, the biotin-labeled cRNA was transcribed *in vitro* from cDNA using a BioArray High-Yield RNA Transcript Labeling kit (ENZO Biochem, New York, NY) and purified again using the RNeasy Mini kit.

Table 3. Microarray Analysis for Top 50 Differentially Expressed Genes between $p53^{WT/WT}$ and $p53^{Val135/WT}$ Mouse Normal Oral Tissues

Genbank	Gene name	Symbol	Fold change ($P < 0.05$) $p53^{WT/WT}/p53^{Val135/WT}$	
			Normal	Tumor
X02578	*Amylase 2, pancreatic*	Amy2	−16.9	
AB021961	*Transformation-related protein 53*	Trp53	−9.6	−14.6
AV380774	*Seminal vesicle secretion 6*	Svs6	−9.4	
AI183084	*Immunoglobulin heavy chain (γ polypeptide)*	Ighg	−7.7	
AA675031	*Transcribed sequence*		−5.9	
AV301321	*Prolyl endopeptidase*	Prep	−5.4	
U03711	*Demilune cell and parotid protein*	Dcpp	−5.3	
X99946	*94-kb Genomic sequence encoding Tsx gene*		−4.8	
AV334462	*Src homology 3 and cysteine-rich domain*	Stac	−4.8	
AV227393	*Thymidine kinase 1*	Tk1	−4.7	
U15976	*Solute carrier family 27, member 1*	Slc27a1	−4.6	
L34808	Caenorhabditis elegans *ceh-10 homeodomain containing homologue*	Chx10	−4.6	
L34570	*Arachidonate 15-lipoxygenase*	Alox15	−4.5	
C76597	*Rho GTPase-activating protein 29*	Arhgap29	−4.4	
AI647632	*Transcribed sequence*		−4.3	
AV209747	*Transcribed sequence*		−4.3	
U30840	*Voltage-dependent anion channel 1*	Vdac1	−4.3	
AV031985	*Guanine nucleotide-binding protein (G protein), γ11*	Gng11	−4.2	
AV063979	*Fatty acid–binding protein 6, ileal (gastrotropin)*	Fabp6	−4.2	
D86603	*BTB and CNC homology 1*	Bach1	−4.2	
U59758	*p53-variant (p53) mRNA*	p53	−4.2	−4.1
AV371942	*Plakophilin 2*	Pkp2	−4.1	
X02801	*Glial fibrillary acidic protein*	Gfap	−4.0	2.0
X05719	*CTL-associated protein 4*	Ctla4	−3.9	
AV232449	*Cadherin 15*	Cdh15	−3.8	2.5
D87271	*ERK2 gene for extracellular signal-regulated kinase 2*	Erk2	2.9	
M55669	*Proprotein convertase subtilisin/kexin type 2*	Pcsk2	3.0	
L32973	*Thymidylate kinase homologue mRNA*		3.0	
D88791	*Cysteine and glycine-rich protein 3*	Csrp3	3.1	
AW122372	*TSPY-like 4, mRNA*		3.1	
AF009513	*Plasma glutamate carboxypeptidase*	Pgcp	3.2	
AV366872	*Selenium-binding protein 1*	Selenbp1	3.2	
AV232606	*Early growth response 2*	Egr2	3.2	
U96401	*Aldehyde dehydrogenase family 1, subfamily A7*	Aldh1a7	3.3	
AV027236	*Insulin-like growth factor–binding protein, acid-labile subunit*	Igfals	3.5	
U75506	*BH3-interacting domain death agonist*	Bid	3.5	
U09181	*Troponin I, cardiac*	Tnni3	3.6	
AB004639	*Fibroblast growth factor 18*	Fgf18	3.6	
M83219	*S100 calcium-binding protein A9 (calgranulin B)*	S100a9	3.9	2.5
AF035717	*Transcription factor 21*	Tcf21	4.0	
L27220	*Neuronal intermediate filament protein (α-internexin) gene*		4.1	
AV002815	*CD68 antigen*	Cd68	4.4	
J03877	*Kallikrein 16*	Klk16	4.5	
J00389	*Kallikrein 26*	Klk26	4.5	
U68058	*Frizzled-related protein*	Frzb	4.7	
U36760	*Forkhead box G1*	Foxg1	5.1	−7.0
AJ224763	*Zinc finger protein 146*	Zfp146	5.2	
X58628	*Kallikrein 13*	Klk13	5.6	
AJ006474	*Ca3 gene 5′-untranslated region and exon 1*		5.8	
X12972	*Myosin alkali light chain (exon 1)*		7.7	−11.6

Affymetrix GeneChip Probe Array and Cluster

The labeled cRNA was applied to the Affymetrix Mu74Av2 GeneChip (Affymetrix, Santa Clara, CA), which contains >12,000 genes and expressed sequence tags on one array according to the manufacturer's recommendations. Every gene or expressed sequence tag is represented by a probe set consisting of ~16 probe pairs (oligonucleotides) of 25-mer oligonucleotides. One sequence of a probe pair represents the complementary strand of the target sequence, whereas the other has a 1-bp mismatch at the central base pair position. This mismatch sequence serves as an internal control for specificity of hybridization.

Four or five independent samples were collected for each group. Array normalization and gene expression estimates were obtained using Affymetrix Microarray Suite version 5.0 software. The array mean intensities were scaled to 1,500. These estimates formed the basis for statistical testing. Differential expression was determined on the combined basis of statistical testing using Student's t test and based on a ratio with a cutoff of $P < 0.05$ and fold change ≥2 called positive for differential expression. For the selected genes, expression indices were transformed across samples to a $N(0,1)$ distribution using a standard statistical Z-transform. These values were put into the GeneCluster program of Eisen et al. (30) and genes were clustered using average linkage and correlation dissimilarity.

Rassf1A Methylation Analysis

The methylation status of the *Rassf1A* promoter region was determined by chemical modification of genomic DNA with

FIGURE 3. MSP analysis of *Rassf1A* in 4NQO-induced tumors. M, presence of methylated *Rassf1A* alleles in tumors; U, presence of unmethylated *Rassf1A* alleles in tumors or normal tissues. *In vitro* methylated DNA (*lane 1*) and normal tissue (*lane 2*) were used as positive and negative controls for *Rassf1A* promoter methylation, respectively. Lanes 3 to 5, representative MSP analysis on tumors from $p53^{WT/WT}$ mice; lanes 6 to 9, representative MSP analysis on tumors from $p53^{Val135/WT}$ mice. H_2O was also included in each reaction as negative control (*lane 10*).

sodium bisulfite and MSP. Bisulfite treatment converts cytosine bases to uracil bases but has no effect on methylcytosine bases. Bisulfite-treated DNA was used as a template for the MSP reaction. Primers for unmethylated reaction were forward 5′-GGTGTTGAAGTTGTGGTTTG-3′ and reverse 5′-TATTATACCCAAAACAATACAC-3′. Primers for methylated reaction were forward 5′-TTTTGCGGTTTCGTTCGTTC-3′ and reverse 5′-CCCGAAACGTACTACTATAAC-3′. The reaction

Table 4. Microarray Analysis for Top 50 Differentially Expressed Genes between $p53^{WT/WT}$ and $p53^{Val135/WT}$ Mouse Oral Tumors

Genbank	Gene name	Symbol	Fold change ($P < 0.05$) $p53^{WT/WT}/p53^{Val135/WT}$	
			Tumor	Normal
AF029843	*Phosphoglycerate mutase 2*	Pgam2	−47.3	
J00453	*IgG-1 gene, D-J-C region*		−31.7	
AJ007971	*IFN-inducible GTPase 1*	Iigp1	−28.8	
M34815	*Chemokine (C-X-C motif) ligand 9*	Cxcl9	−21.1	
L38444	*T-cell-specific GTPase*	Tgtp	−20.3	
X15662	*Cytokeratin endo A (no 8) 5′ end*		−16.3	
U90926	*Putative tumor necrosis factor resistance-related protein mRNA*		−14.8	
AB021961	*Transformation-related protein 53*	Trp53	−14.6	−9.6
U53219	*IFN-γ-induced GTPase*	Igtp	−13.4	
AI850363	*Muscle glycogen phosphorylase*	Pygm	−12.5	
X12972	*Myosin alkali light chain (exon 1)*		−11.6	7.7
U73037	*IFN-regulatory factor 7*	Irf7	−11.5	
AJ007970	*Guanylate nucleotide-binding protein 2*	Gbp2	−11.3	
AF035643	*Vesicle-associated membrane protein 5*	Vamp5	−11.1	
X67140	*SR calcium ATPase*		−11.1	−1.8
AI854020	*Cysteine dioxygenase 1, cytosolic*	Cdo1	−11.0	
AF062476	*Stimulated by retinoic acid gene 6*	Stra6	−10.4	
AJ132098	*Vanin 1*	Vnn1	−10.3	
AJ223361	*Myosin, heavy polypeptide 4, skeletal muscle*	Myh4	−10.3	−1.9
X16009	*Mitogen-regulated protein/proliferin (MRP/PLF), exon 1*		−10.1	−2.5
M63630	*IFN-γ-inducible protein*	Ifi47	−9.3	
X99915	*HMGI-C gene*		−9.2	
AW047476	*Guanylate nucleotide-binding protein 3*	Gbp3	−8.8	
AB008174	*Transcription factor 2*	Tcf2	−7.7	
L48989	*Troponin T3, skeletal, fast*	Tnnt3	−7.6	
AI182588	*Carboxypeptidase N, polypeptide 1*	Cpn1	5.3	
Y07812	*Myelin and lymphocyte protein, T-cell differentiation protein*	Mal	5.5	
M24264	*Testosterone 16α-hydroxylase (CC) gene*		5.5	
J05177	*Mast cell protease 2*	Mcpt2	5.6	
X15789	*Cellular retinoic acid-binding protein I*	Crabp1	5.6	−2.1
AI844839	*RIKEN cDNA 6330442E10 gene*		5.8	
AJ005566	*Small proline-rich protein 2H*	Sprr2h	5.8	
D30782	*Epiregulin*	Ereg	6.0	
D86424	*Keratin-associated protein 3-1*	Krtap3-1	6.0	
AI645662	*Keratin-associated protein 3-3*	Krtap3-3	6.1	−2.3
X97986	*Desmocollin 1*	Dsc1	6.1	
AA607761	*DNase 1-like 2*	Dnase1l2	6.3	
M27695	*Urate oxidase*	Uox	6.4	
X80417	*Potassium inwardly rectifying channel, subfamily J, member 12*	Kcnj12	7.0	
AF011418	*Vomeronasal 2, receptor, 8*	V2r8	7.1	
AF053235	*Keratin complex 1, acidic, gene 16*	Krt1-16	7.4	
AJ005569	*SPRR2K gene*		8.1	
AA615849	*Single WAP motif protein 2*	Swam2	10.3	
AV027999	*F-box only protein 3*	Fbxo3	12.0	
AV230260	*Expressed sequence AL033326*	AL033326	12.6	
AJ242830	*HemT gene, exons 1-3*		17.4	
AF031485	*Keratin-associated protein 13*	Krtap13	26.4	−2.2
M36780	*Casein α*	Csna	31.6	−2.0
X65506	*Keratin complex 1, acidic, gene 5*	Krt1-5	36.0	−2.1
X65505	*Keratin complex 2, basic, gene 16*	Krt2-16	206.8	

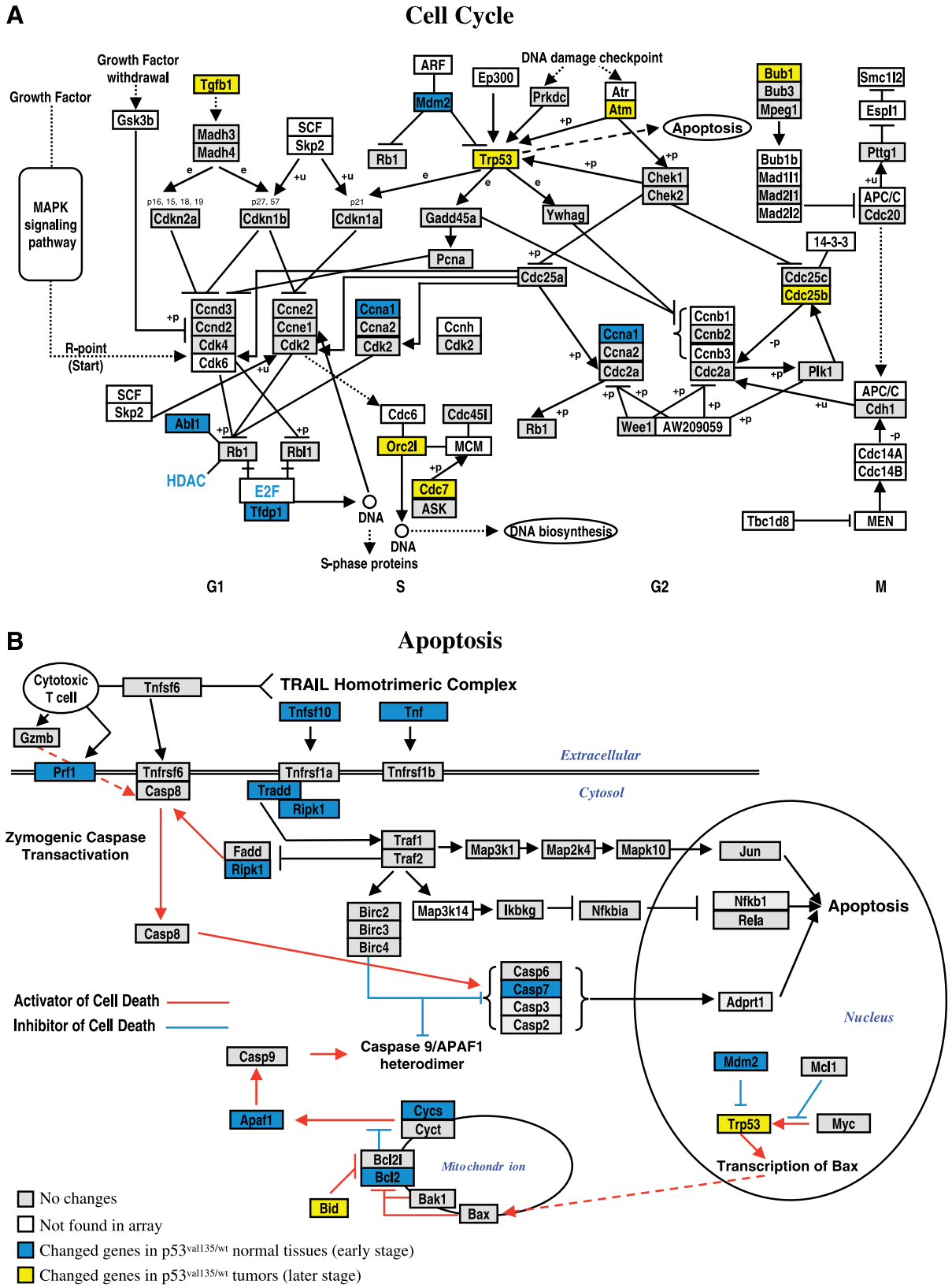

FIGURE 4. **A** and **B.** GenMAPP cell cycle regulation and apoptosis pathways integrate the expression data (cutoff of $P < 0.05$; fold change >1.5). Yellow, changes found in normal tissues from the $p53^{Val135/WT}$ mice; blue, changes found in 4NQO-induced $p53^{Val135/WT}$ tumors when compared with those from $p53^{WT/WT}$ mice; gray, the selection criteria were not met, but the gene is represented on the array. White boxes, the gene was not present on the chip.

was incubated at 95°C for 1 minute, 55°C for 1 minute, and 72°C for 1 minute for 35 cycles. The methylation fragment was 213 bp, and the nonmethylation fragment was 204 bp. DNA from normal skin was used as a control for unmethylated *Rassf1A*, and normal skin DNA treated with *Sss*I methyltransferases was used as a control for methylated *Rassf1A*. H_2O was used as negative control. Each PCR (25 μL) was loaded onto a 6% nondenaturing polyacrylamide gel, stained with ethidium bromide, and pictured under UV light.

GenMAPP

Signal transduction pathways, metabolic pathways, and other functional groupings of genes were evaluated for differential regulation using the visualization tool GenMAPP (University of California at San Francisco; http://www.genmapp.org). GenMAPP is a recently reported tool for visualizing expression data in the context of biological pathways (31). We imported the statistical results of our data set into the program and used GenMAPP to illustrate pathways containing differentially expressed genes. Differential gene expression was based on p53 genotype status ($P < 0.05$; fold change >1.5).

Statistical Analysis

Fisher's exact test was used to determine the difference in incidence between $p53^{Val135/WT}$ and $p53^{WT/WT}$ mice. Nonparametric Wilcoxon's rank-sum test was used to determine the difference in tumor multiplicity between $p53^{Val135/WT}$ and $p53^{WT/WT}$ mice.

Acknowledgments

We thank Dr. Roger W. Wiseman for providing the p53 transgenic mice and Drs. Daolong Wang and William J. Lemon for statistical assistance. Raw data are available upon request.

References

1. Greenlee RT, Hill-Harmon MB, Murray T, Thun M. Cancer statistics. CA Cancer J Clin 2001;51:15–36.

2. Jovanovic A, Schulten EA, Kostense PJ, Snow GB, van der Waal I. Tobacco and alcohol related to the anatomical site of oral squamous cell carcinoma. J Oral Pathol Med 1993;22:459–62.

3. Sugerman PB, Joseph BK, Savage NW. Review article: The role of oncogenes, tumour suppressor genes and growth factors in oral squamous cell carcinoma: a case of apoptosis versus proliferation. Oral Dis 1995;*1*:172–88.

4. Califano J, van der Riet P, Westra W, et al. Genetic progression model for head and neck cancer: implications for field cancerization. Cancer Res 1996;56:2488–92.

5. Field JK. Oncogenes and tumour-suppressor genes in squamous cell carcinoma of the head and neck. Eur J Cancer B Oral Oncol 1992;28B:67–76.

6. Greenblatt MS, Bennett WP, Harris CC. Mutations in the p53 tumor suppressor gene: clues to cancer etiology and molecular pathogenesis. Cancer Res 1994;54:4855–78.

7. Harris CC. p53 tumor suppressor gene: at the crossroads of molecular carcinogenesis, molecular epidemiology, and cancer risk assessment. Environ Health Perspect 1996;104 Suppl 3:435–9.

8. Li FP, Fraumeni JF, Jr. Soft-tissue sarcomas, breast cancer, and other neoplasms. A familial syndrome? Ann Intern Med 1969;71:747–52.

9. Zhang Z, Liu Q, Lantry LE, et al. A germline p53 mutation accelerates pulmonary tumorigenesis: p53-independent efficacy of chemopreventive agents green tea or dexamethasone/myo-inositol and chemotherapeutic agents Taxol or Adriamycin. Cancer Res 2000;60:901–7.

10. Zhang Z, Li J, Lantry LE, et al. M, p53 transgenic mice are highly susceptible to 1,2-dimethylhydrazine-induced uterine sarcomas. Cancer Res 2002;62:3024–9.

11. Wang Y, Zhang Z, Kastens E, Lubet RA, You M. Mice with alterations in both p53 and Ink4a/Arf display a striking increase in lung tumor multiplicity and progression: differential chemopreventive effect of budesonide in wild-type and mutant A/J mice. Cancer Res 2003;63:4389–95.

12. Zhang Z, Wang Y, Lantry LE, et al. Farnesyltransferase inhibitors are potent lung cancer chemopreventive agents in A/J mice with a dominant-negative p53 and/or heterozygous deletion of Ink4a/Arf. Oncogene 2003;22:6257–65.

13. Ahomadegbe JC, Barrois M, Fogel S, et al. High incidence of p53 alterations (mutation, deletion, overexpression) in head and neck primary tumors and metastases; absence of correlation with clinical outcome. Frequent protein overexpression in normal epithelium and in early non-invasive lesions. Oncogene 1995;10:1217–27.

14. Brennan JA, Boyle JO, Koch WM, et al. Association between cigarette smoking and mutation of the p53 gene in squamous-cell carcinoma of the head and neck. N Engl J Med 1995;332:712–7.

15. Erber R, Conradt C, Homann N, et al. Bosch FX, TP53 DNA contact mutations are selectively associated with allelic loss and have a strong clinical impact in head and neck cancer. Oncogene 1998;16:1671–9.

16. Liloglou T, Scholes AG, Spandidos DA, Vaughan ED, Jones AS, Field JK. p53 mutations in squamous cell carcinoma of the head and neck predominate in a subgroup of former and present smokers with a low frequency of genetic instability. Cancer Res 1997;57:4070–4.

17. Casey G, Lopez ME, Ramos JC, et al. DNA sequence analysis of exons 2 through 11 and immunohistochemical staining are required to detect all known p53 alterations in human malignancies. Oncogene 1996;13:1971–81.

18. Zhang Y, Xiong Y. Mutations in human ARF exon 2 disrupt its nucleolar localization and impair its ability to block nuclear export of MDM2 and p53. Mol Cell 1999;3:579–91.

19. Hawkins BL, Heniford BW, Ackermann DM, Leonberger M, Martinez SA, Hendler FJ. 4NQO carcinogenesis: a mouse model of oral cavity squamous cell carcinoma. Head Neck 1994;16:424–32.

20. Steidler NE, Reade PC. Experimental induction of oral squamous cell carcinomas in mice with 4-nitroquinoline-1-oxide. Oral Surg Oral Med Oral Pathol 1984;57:524–31.

21. Yuan B, Heniford BW, Ackermann DM, Hawkins BL, Hendler FJ. Harvey ras (H-ras) point mutations are induced by 4-nitroquinoline-1-oxide in murine oral squamous epithelia, while squamous cell carcinomas and loss of heterozygosity occur without additional exposure. Cancer Res 1996;54:5310–7.

22. Ohne M, Satoh T, Yamada S, Takai H. Experimental tongue carcinoma of rats induced by oral administration of 4-nitroquinoline 1-oxide (4NQO) in drinking water. Oral Surg Oral Med Oral Pathol 1985;59:600–7.

23. Hartwell LH, Kastan MB. Cell cycle control and cancer. Science 1994;266:1821–8.

24. Donehower LA, Harvey M, Slagle BL, et al. Mice deficient for p53 are developmentally normal but susceptible to spontaneous tumors. Nature 1992;356:215–21.

25. Meyer JS, He W. High proliferative rates demonstrated by bromodeoxyuridine labeling index in breast carcinomas with p53 overexpression. J Surg Oncol 1994;56:146–52.

26. Gallo O, Sardi I, Pepe G, et al. Multiple primary tumors of the upper aerodigestive tract: is there a role for constitutional mutations in the p53 gene? Int J Cancer 1999;82:180–6.

27. Rowley H, Sherrington P, Helliwell TR, Kinsella A, Jones AS. p53 expression and p53 gene mutation in oral cancer and dysplasia. Otolaryngol Head Neck Surg 1998;118:115–23.

28. Qin GZ, Park JY, Chen SY, Lazarus P. A high prevalence of p53 mutations in pre-malignant oral erythroplakia. Int J Cancer 1999;80:345–8.

29. Ide F, Kitada M, Sakashita H, Kusama K, Tanaka K, Ishikawa T. p53 haploinsufficiency profoundly accelerates the onset of tongue tumors in mice lacking the xeroderma pigmentosum group A gene. Am J Pathol 2003;163:1729–33.

30. Eisen MB, Spellman PT, Brown PO, Botstein D. Cluster analysis and display of genome-wide expression patterns. Proc Natl Acad Sci U S A 1998;95:14863–8.

31. Dahlquist KD, Salomonis N, Vranizan K, Lawlor SC, Conklin BR. GenMAPP, a new tool for viewing and analyzing microarray data on biological pathways. Nat Genet 2002;31:19–20.

Correction: Article on the Effect of Germ-line p53 Mutation on Oral Carcinogenesis

In the article on the effect of germ-line p53 mutation on oral carcinogenesis in the June 2006 issue of *Molecular Cancer Research*, one of the authors, Jie Li, was inadvertently omitted.

Zhang Z, Wang Y, Yao R, Li J, Lubet RA, Ming Y. p53 Transgenic mice are highly susceptible to 4-nitroquinoline-1-oxide-induced oral cancer. Mol Cancer Res 2006; 4:401–10.

doi:10.1158/1541-7786.MCR-4-8-COR

Molecular Cancer Research

p53 Transgenic Mice Are Highly Susceptible to 4-Nitroquinoline-1-Oxide-Induced Oral Cancer

Zhongqiu Zhang, Yian Wang, Ruisheng Yao, et al.

Mol Cancer Res 2006;4:401-410.